AN INVESTIGATION ON STRESS CORROSION CRACKING (SCC) BEHAVIOUR OF Cr-Mo STEELS

Hong Youshi* and Liang Kiaming**

**Institute of Mechanics, Chinese Academy of Sciences, Beijing, China*
***Qinghua University, Beijing, China*

ABSTRACT

The effects of carbon content and tempering temperature on stress corrosion cracking (SCC) property of Cr-Mo structural steels in 3.5% NaCl aqueous solution have been investigated. It is shown that low carbon Cr-Mo structural steel which has been quenched and tempered at about 200°C presents better combination of strength and toughness than middle carbon one with the same yield strength level. Middle carbon Cr-Mo steel presents high SCC susceptibility although it has been tempered at 400°C. There is a temper embrittlement zone near 320°C where high SCC susceptibility is displayed. SCC property is markedly affected by carbon content. There is an approximately linear relationship between K_{1scc} and $f^{-1/6}$ (f is the volume fraction of carbide). The mechanism of SCC and an estimated model are discussed as well.

KEYWORDS

Stress corrosion cracking (SCC); Cr-Mo structural steel; tempering temperature; carbon content; hydrogen assisted cracking (HAC); K_{1scc}.

INTRODUCTION

Previous studies have elementarily reported the effects of carbon content on stress corrosion cracking (SCC) property of structural steels (Sandoz, 1971; Wang, Tang and Li, 1982). In order to select reasonably the carbon content and tempering system of low alloy structural steel used in aqueous engineering environment, it is necessary to further investigate the effects of carbon content and tempering temperature on SCC property, so as to obtain a better combination of strength and toughness (including K_{1c} and K_{1scc}) at the yield strength level needed. The present paper attempts to investigate the effects of carbon content and tempering temperature on the SCC property of Cr-Mo system structural steels with different carbon content. Moreover, the mechanism of SCC and an estimated model are discussed.

EXPERIMENTAL PROCEDURE

Materials

Four steels were used in this work. The chemical compositions are listed in Table 1. The specimens of each steel were quenched and then tempered for one hour at 200°C, 280°C, 320°C, 400°C, 500°C and 620°C, respectively. The yield strength, σ_y, and the fracture toughness, K_{1c}, are shown in Figs. 1 and 2, which were reported by Hong and others (1981).

TABLE 1 Chemical Compositions of Test Steels (wt. %)

Steel	C	Si	Mn	P	S	Cr	Mo	Fe
A	0.14	0.31	0.50	0.017	0.016	0.90	0.48	Balance
B	0.21	0.28	0.53	0.014	0.008	0.91	0.20	Balance
C	0.29	0.33	0.53	0.017	0.009	0.90	0.28	Balance
D	0.35	0.30	0.51	0.017	0.011	0.92	0.23	Balance

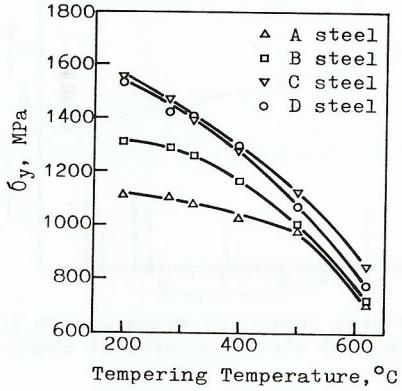

Fig. 1. Variation of σ_y with tempering temperature.

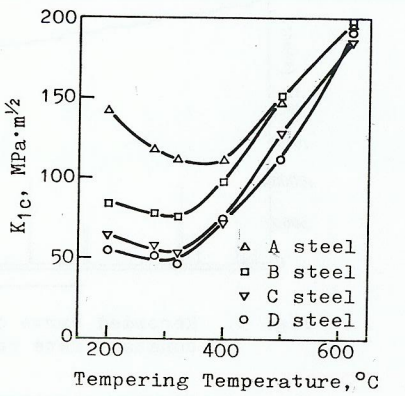

Fig. 2. Variation of K_{1c} with tempering temperature.

SCC Test

Stress corrosion cracking test was performed on precracked bend specimens (thickness 20mm, width 40mm and length 190mm) in 3.5% NaCl aqueous solution by means of the cantilever beam method (Brown, 1966). The temperature of the solution was controlled at 28°C. The threshold value of stress intensity factor, K_{1scc}, was measured in this experiment. When the crack growth occurred above K_{1scc}, the displacement at the end of cantilever beam and the acoustic emission (AE) count were recorded using an X-Y recorder. The probe of the AE device was installed near the crack. It is considered that the length of crack propagation is proportional to the displacement at the end of cantilever beam so far as the crack growth is within a limited range. By this way the constant crack growth rate, V_a, was also measured.

Diffused Hydrogen Determination

The sample (55x20x10mm) cut from the SCC test specimen was charged with hydrogen for 40 minutes in the solution of (5% H_2SO_4 + 200mg/l As_2O_3). The current density is 0.1mA per square millimetre of the sample surface area. Then this sample was put inside a gas collector which was placed in a container filled with glycerine. This set was put in a constant temperature cabinet at 30°C. The over saturated hydrogen may escape from the sample and spread into the gas collector. The scale reading shown on the collector presents the amount of the diffused hydrogen. It was noted down until hydrogen stopped escaping. The diffused hydrogen amount per unit weight of the sample (DHA) is obtained from the latest reading value. DHA may be used to represent approximately the hydrogen solubility of the sample.

Fractography

The fracture surfaces of SCC specimens were examined by scanning electron microscopy (SEM). The crack profiles of these specimens were observed by optical microscopy.

RESULTS AND DISCUSSION

Effects of Carbon Content and Tempering Temperature on SCC Property

Figures 3 and 4 show the SCC experimental results of the steels tested. It is seen that, in general, the SCC resistance increases with the increasing of tempering temperature above 320°C, and there is a temper embrittlement zone near 320°C where K_{1scc} decreases and V_a increases. Figure 5 shows that the K_1 range where crack growth rate is independent of K_1 is related to tempering temperature.

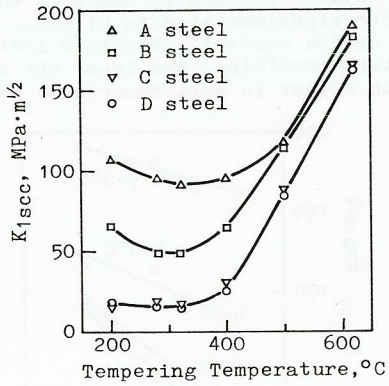

Fig. 3. Variation of K_{1scc} with tempering temperature.

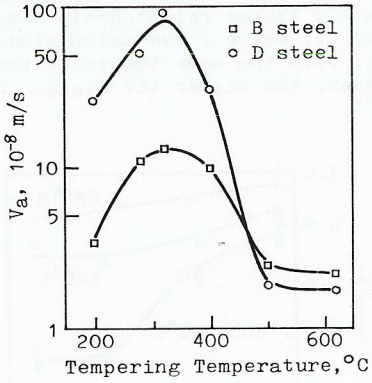

Fig. 4. Variation of V_a with tempering temperature.

The effects of carbon content and tempering temperature on SCC property are investigated with either the same yield strength level condition or the same tempering temperature condition. Firstly, for the same yield strength

level within 1100-1300MPa, both K_{1scc} and K_{1c} of low carbon Cr-Mo steel tempered at 200°C are higher than those of middle carbon one (Fig. 6). When σ_y is within 700-1000MPa (tempered at above 500°C), the difference in K_{1scc} or K_{1c} between these steels gradually decreases and finally diminishes. Furthermore, both K_{1scc} and K_{1c} reach a high level in this yield strength range. If certain values of K_{1scc} and K_{1c} are ensured, however, middle carbon Cr-Mo steel may possess higher yield strength than low carbon one when both were tempered at the same tempering temperature above 500°C.

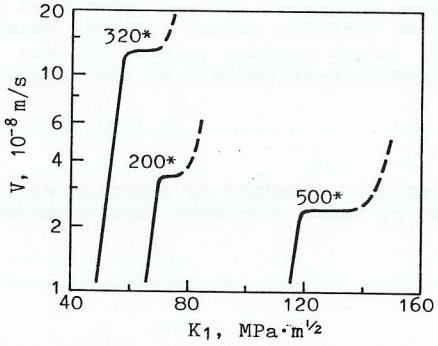

Fig. 5. Crack growth rate in B steel vs K_1.
*Tempering temperature

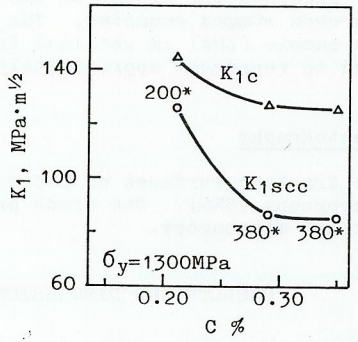

Fig. 6. Effect of carbon content on K_{1scc} and K_{1c}.
*Tempering temperature

Secondly, at the same tempering temperature, low carbon Cr-Mo steel exhibits lower SCC susceptibility than middle one (Fig. 7) if the ratio of K_{1scc} to K_{1c} is regarded as an expression of SCC susceptibility. In this condition, it is considered that the difference in mechanical property of the Cr-Mo steels tested is mainly caused by carbon content or volume fraction of carbide, f. Like the relationship between K_{1c} and f, there is an approximately linear relationship between our experimental data of K_{1scc} and $f^{-1/6}$ (Fig. 8), where f was calculated from carbon content. Figure 8 indicates that, with the same tempering temperature condition, the lower the carbon content, the higher the K_{1scc}. Such an effect is more remarkable below 400°C.

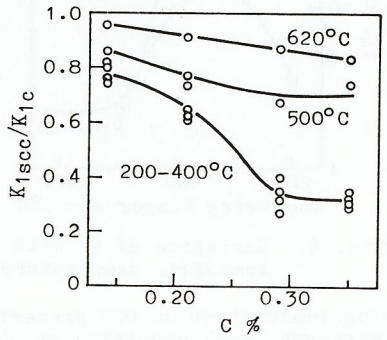

Fig. 7. K_{1scc}/K_{1c} vs carbon content.

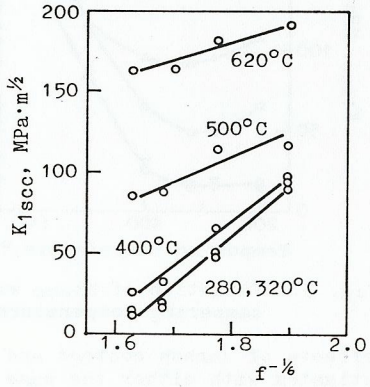

Fig. 8. K_{1scc} vs $f^{-1/6}$.

SCC Mechanism in NaCl Aqueous Solution

It is known that, in the process of hydrogen assisted cracking (HAC), hydrogen may be produced at the crack tip when the specimen is loaded and immersed in corrosive solution. Then hydrogen diffuses and concentrates towards the high triaxial stress region near the crack tip. Consequently, the crack propagates a unit of length while a critical hydrogen concentration is reached. Soon afterwards, hydrogen again diffuses and concentrates towards the new crack tip and there is an incubation before a new crack is formed. Such a process continues until the final fracture takes place. Thus, if SCC is controlled by HAC, the apparent behaviour should be that a given material possesses its K_{1scc} and that stress corrosion crack propagates in the way of step by step. As mentioned above, the steels studied do possess their K_{1scc} in 3.5% NaCl aqueous solution. Moreover, we observed that the recorded results display the propagation of stress corrosion crack is discontinuous and so is AE count monitored. Figure 9 is an example of B steel. From the observation on crack profiles, the isolated crack in front of crack tip is observed in most of specimens. It is also a phenomenon of discontinuous crack growth. Figure 10 is an example of D steel.

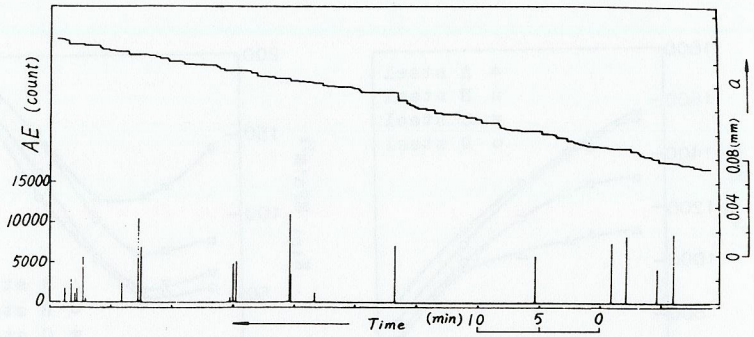

Fig. 9. Recorded curve of stress corrosion crack growth in constant rate region of B steel tempered at 280°C.

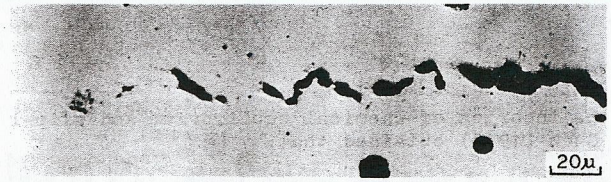

Fig. 10. Profile photograph of D steel tempered at 500°C.

Figure 11 shows what the SEM observing results on the initiation zone of stress corrosion crack are related to carbon content, tempering temperature, and K_{1scc}. It is clearly that

$$K_{1scc(TD)} > K_{1scc(TQC)} > K_{1scc(IG)}$$

where TD is transgranular dimple, TQC transgranular quasi-cleavage, and IG intergranular cleavage. This result agrees with what the fractography varies with K_1 in HAC which was reported by Beachem (1972). Summing up the

above facts, it is seen that our experimental investigation supports that the SCC mechanism of high strength low alloy structural steel in NaCl aqueous solution is HAC.

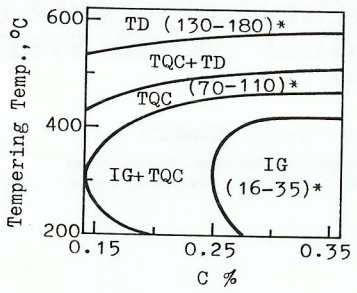

Fig. 11. Illustration of fractography observing results. *K_{1scc} (MPa·m½)

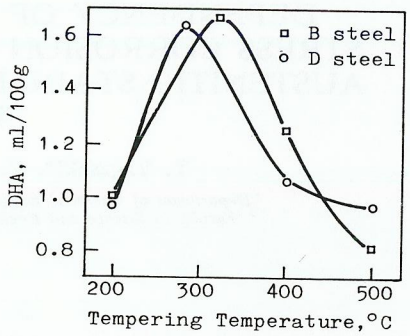

Fig. 12. Diffused hydrogen amount per unit weight (DHA) vs tempering temperature.

Figure 12 shows the results of diffused hydrogen determination of B and D steels. In the temper embrittlement zone (near 320°C), DHA reaches its maximum value. This result is consistent with the systematic results reported by Newman and Shreir (1969). They considered that such a phenomenon is resulted from different amount of interface area between carbide and ferrite. The interface area provides traps for the accumulation of hydrogen and the area amount depends on tempering temperature. The maximum value of DHA appeared in temper embrittlement zone should be referred to the maximum amount of interface area which is resulted from the formation of great amount of cementite which is incoherent from ferrite. Obviously, the larger the amount of DHA, the easier the accumulation of hydrogen. As a result, the concentration of hydrogen near crack tip quickly reaches its critical value. Besides, the effect of impurity can be superposed on that of hydrogen (McMahon, Briant and Banerji, 1977). What is mentioned above is referred to the temper embrittlement zone near 320°C where high SCC susceptibility is displayed.

An Estimated Model

According to the theories of chemical equilibrium and slip-line field, Gerberich and Chen (1975) obtained that:

$$K_{1scc} = \frac{RT}{\alpha V} \ln\left(\frac{Cc}{Co}\right) - \frac{\sigma_y}{2\alpha} \qquad (1)$$

They postulated that:

$$\frac{Cc}{Co} = \frac{\beta}{\sigma_y} \qquad (2)$$

where C_c is the critical value of hydrogen concentration, C_o the equilibrium hydrogen concentration in the unstressed lattice, and β a constant. Then, they proposed a model to estimate K_{1scc} of structural steel of which the crack growth occurs by HAC. That is:

$$K_{1scc} = \frac{RT}{\alpha V} \ln\left(\frac{\beta}{\sigma_y}\right) - \frac{\sigma_y}{2\alpha} \qquad (3)$$

where R is gas constant (8.314×10^{-6} MN·m/K·mol), T absolute temperature, V the molar volume of hydrogen in Fe (2×10^{-6} m^3/mol), and $\alpha=13m^{-1/2}$. For low alloy structural steel they let β=3170MPa. They showed that Eqn. (3) fitted some results of structural steels. In fact, Eqn. (3) is an empiric formula which relates K_{1scc} to σ_y at a given condition. However, not only does K_{1scc} depend on σ_y but also on some material parameters. Equation (3) may fit certain results but in some other cases there is a large difference between estimated value and tested one just like ours (Fig. 13). Since there is an approximately linear relationship between K_{1scc} and $f^{-1/6}$ (Fig. 8) we postulated that:

$$\frac{Cc}{Co} = \left(\frac{\beta'}{\sigma_y}\right) f^{-1/6} \qquad (4)$$

Then, $$K_{1scc} = f^{-1/6} \left(\frac{RT}{\alpha V}\right) \ln\left(\frac{\beta'}{\sigma_y}\right) - \frac{\sigma_y}{2\alpha} \qquad (5)$$

where we let β'=2480MPa. Equation (5) fits the present results quite well (Fig. 13) except that of the temper embrittlement zone (TEZ). In there interreactions take place among carbide, impurity and hydrogen, and fracture fractography is different from that outside the TEZ. If we let β'=2220MPa, then Eqn. (5) also fits the results of that zone (Fig. 13). That is:

$$\beta' = \begin{cases} 2480 \text{ MPa} & \text{(Outside the TEZ)} \\ 2220 \text{ MPa} & \text{(In the TEZ)} \end{cases}$$

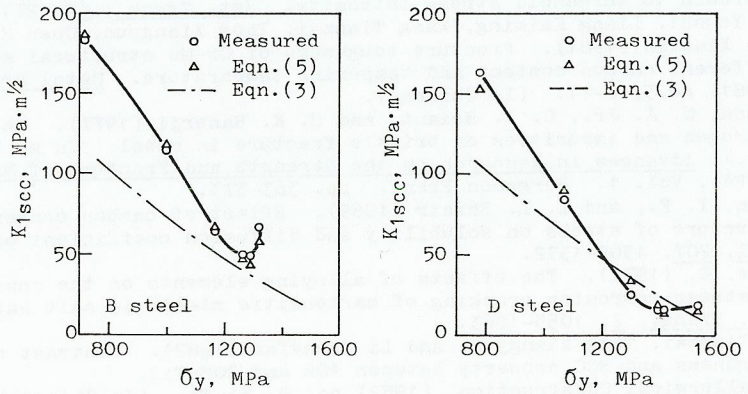

Fig. 13. Contrast between estimated and measured value of K_{1scc}.

CONCLUSIONS

1. Low carbon Cr-Mo steel which was quenched and tempered at about 200°C exhibits better combination of strength and toughness in the yield strength level ranging from 1100-1300MPa. Middle carbon Cr-Mo steel which was quenched and tempered over 550°C exhibits good combination of strength and toughness in the yield strength level ranging from 700-1000MPa, but it presents high SCC susceptibility even tempered at 400°C.
2. There is a temper embrittlement zone near 320°C where Cr-Mo steel

displays low K_{1scc} and K_{1c} with high V_a and DHA.

3. The present investigation supports that SCC of low alloy structural steel in NaCl aqueous solution is caused by HAC.
4. SCC property is markedly affected by carbon content. There is an approximately linear relationship between K_{1scc} and $f^{-1/6}$. So, we reform the Gerberich-Chen fomula as:

$$K_{1scc} = f^{-1/6} \left(\frac{RT}{\alpha V}\right) \ln\left(\frac{\beta'}{\sigma_y}\right) - \frac{\sigma_y}{2\alpha} \qquad (5)$$

and $$\beta' = \begin{cases} 2480 \text{ MPa} & \text{(Outside the TEZ)} \\ 2220 \text{ MPa} & \text{(In the TEZ)} \end{cases}$$

Equation (5) fits the present experimental results quite well.

ACKNOWLEDGEMENT

The authors are grateful to Professors Chen Nanping, Wang Tianzai and Tang Xiangyun for their valuable guidance, and to Drs. Zhang Shuangyin and G. C. Li for their helpful discussions.

REFERENCES

Beachem, C. D. (1972). A new model for hydrogen-assisted cracking (hydrogen "embrittlement"). Met. Trans., 3, 437-451.

Brown, B. F. (1966). A new stress-corrosion cracking test for high-strength alloys. Materials Research and Standards, 6, 129-133.

Gerberich, W. W., and Y. T. Chen (1975). Hydrogen-controlled cracking—an approach to threshold stress intensity. Met. Trans., 6A, 271-278.

Hong Youshi, Liang Kaiming, Wang Tianzai, Tang Xiangyun, Chen Nanping, and Xia Xiaoxin (1981). Fracture toughness of Cr-Mo structural steels with different carbon content and tempering temperature. Metal Products, (1981) no.5, 6-11. (In Chinese).

McMahon, C. J. Jr., C. L. Briant, and S. K. Banerji (1977). The effects of hydrogen and impurities on brittle fracture in steel. In M. R. Taplin (Ed.), Advances in Research on the Strength and Fracture of Materials, (ICF4), Vol. 1. Pergamon Press. pp. 363-373.

Newman, I. F., and L. L. Shreir (1969). Effect of carbon content and structure of steels on solubility and diffusion coefficient of hydrogen. JISI, 207, 1369-1372.

Sandoz, G. (1971). The effects of alloying elements on the susceptibility to stress-corrosion cracking of martensitic steels in salt water. Met. Trans., 2, 1055-1063.

Wang Tianzai, Tang Xiangyun, and Li Shengfan (1982). Contrast of fracture toughness and SCC property between 40B and 20MnTiB. Metallurgical Construction, (1982) no. 8, 31-37. (In Chinese).